angle of 40° across samples) against the thickness also indicated the polar nature of the material.

16. G. N. Tew, L. M. Li, S. I. Stupp, *J. Am. Chem. Soc.* **120**, 5601 (1998).
17. ¹H NMR spectra revealed the disappearance of 70% of the vinyl protons after annealing precursor **1** and after isolating the macromolecular product of narrow MW distribution. The disappearance of vinyl protons [δ4.8 to δ5.9 parts per million (ppm)] is accompanied by an increase of 20% in the number of aliphatic protons. These changes reflect the conversion of double to single bonds and are consistent with the

expected values. The position of all the aromatic, aliphatic, and residual vinyl peaks were found to be the same after the transformation from precursor **1** to macromolecular objects. However, some broadening and suppression of aromatic resonances were observed (δ7.3 to δ8.5 ppm).
18. L. Song *et al.*, *Science* **274**, 1859 (1996); Y. Fang, S. Cheley, H. Bayley, J. Yang, *Biochemistry* **36**, 9518 (1997); S. Cheley *et al.*, *Protein Eng.* **10**, 1433 (1997).
19. B. Walker and H. Bayley, *J. Biol. Chem.* **270**, 23065 (1995); R. G. Panchal and H. Bayley, *ibid.*, p. 23072; H. Bayley, *Bioorg. Chem.* **23**, 340 (1995).

Compensation of Horizontal Temperature and Salinity Gradients in the Ocean Mixed Layer

Daniel L. Rudnick* and Raffaele Ferrari

Establishment of the temperature-salinity relationship in the ocean has concerned oceanographers for decades because of its importance for understanding ocean circulation. High-resolution measurements in the ocean mixed layer are used to show that temperature and salinity gradients on horizontal scales of 20 meters to 10 kilometers tend to compensate in their effect on density. These observations support the notion of a horizontal mixing in the mixed layer that depends on density gradient.

Temperature and salinity are the two most important physical properties of seawater. First, temperature and salinity determine the dynamic variable density at fixed pressure. Second, our understanding of the general circulation of the ocean is based to a large extent on the use of temperature and salinity as tracers to infer the flow. The temperature-salinity relationship has therefore been an object of study since the early days of oceanography. Iselin (*1*) noticed the correspondence between horizontal profiles in the surface mixed layer (*2*) and vertical profiles in the thermocline (*3*) and concluded that subsurface water is derived from late winter surface water. Properties set in the winter mixed layer remain essentially unchanged as water is transported along surfaces of constant density (*4, 5*). Direct observations of small vertical diffusivities in the thermocline (*6, 7*) support the idea that water properties are set at the ocean's surface and bottom boundaries. The question of how the temperature-salinity relationship is established in the mixed layer is thus of central importance to oceanography. Further, this relationship is of climatic importance because coupling of the atmosphere and ocean takes place through the mixed layer, and it is of biological importance because biomass in

the ocean is concentrated in the upper ocean where sufficient sunlight is available for photosynthesis.

A measure of the relative effect of temperature and salinity on density is the density ratio

$$R \equiv \frac{\alpha \Delta \theta}{\beta \Delta S} \qquad (1)$$

where α and β are the expansion coefficients for temperature and salinity, and the temperature and salinity differences $\Delta\theta$ and ΔS are taken over a spatial interval. A horizontal front that is cold and fresh on one side and warm and salty on the other, so that temperature and salinity have opposing effects on density, is often said to be compensated, having a density ratio of 1. The phenomenon of compensation is well known at certain fronts (*8, 9*). A front where the effect of temperature on density is twice (but opposite) that of salinity, and hence density varies across the front, has a density ratio of 2.

The last published works of Stommel (*10, 11*) suggest a regulating mechanism for the temperature-salinity relationship in the mixed layer. Stommel observes that the mixed-layer
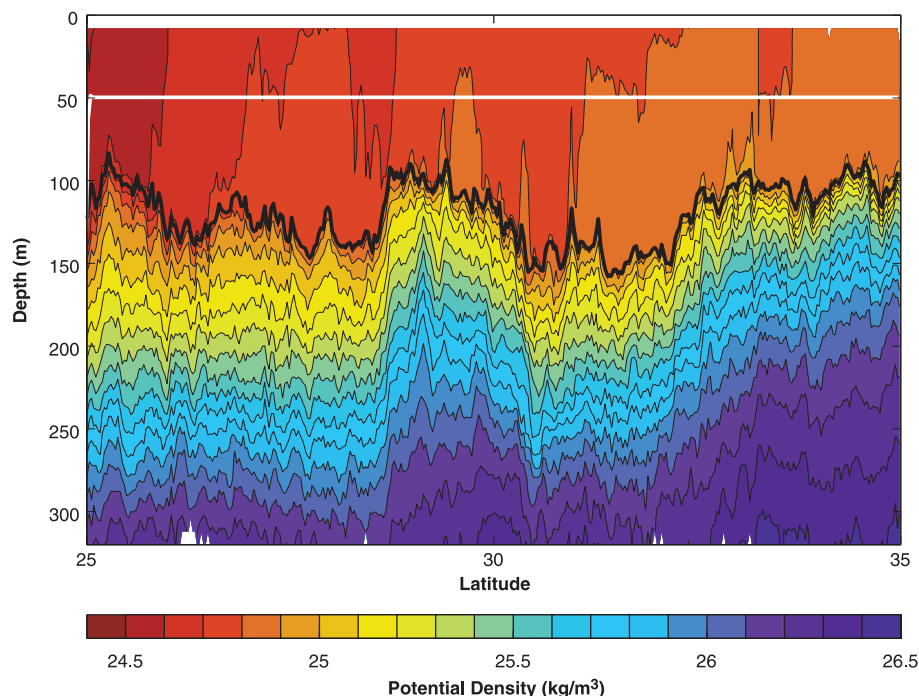

Fig. 1. Potential density section along 140°W as measured by a sawtooth SeaSoar tow. Data are averaged in bins 3 km in the horizontal by 8 m in the vertical before contouring. The white line is a level tow along the 50-dbar surface. The mixed layer as defined by a 0.1 kg m⁻³ difference from the shallowest measurement is indicated by the black line. Mixed-layer depth varies between 100 and 150 dbar, so 50 dbar is always within the mixed layer.

Scripps Institution of Oceanography, La Jolla, CA 92093–0230, USA.

*To whom correspondence should be addressed. E-mail: drudnick@ucsd.edu

density ratio is about 2 in the latitude range of 20° to 50° of all oceans. Stommel explains this observation with a simple two-box model in which temperature is held at or relaxed to a linear gradient, salinity is forced stochastically (as in the case of forcing by rainstorms), and a horizontal mass exchange between the two boxes is a function of the density gradient. The result is that, on average, the density ratio of 2 is reached if the mass exchange is proportional to the absolute value of the density gradient.

Related models by Young and collaborators (*12–14*) suggest that the horizontal diffusivity in the mixed layer should be parameterized as proportional to the density gradient squared—in accord with Stommel's mass exchange, albeit with a different functional dependence. The physical explanation of this parameterization is as follows. Suppose that the temperature and salinity of a vertically mixed layer were randomly distributed. At some locations temperature and salinity gradients would compensate each other exactly, whereas at other locations they would create very strong horizontal density gradients; much of the mixed layer would lie between these extremes. The strong density gradients tend to slump as a result of gravity—that is, isopycnals tilt from the vertical to the horizontal (*15*). Any subsequent vertical mixing results in a weakening horizontal density gradient. This mechanism is essentially a horizontal shear dispersion, where the shear results from slumping density gradients and vertical mixing results from the variety of processes that mix the mixed layer. Those temperature-salinity fronts that are compensated do not slump and therefore do not experience horizontal dispersion. The net result is that density fronts are diffused whereas compensated fronts persist, and a density ratio of 1 is achieved.

The goal of this study was to quantify the variability of temperature and salinity in the mixed layer on horizontal scales of 10 m to 100 km and to evaluate the Stommel and Young models discussed above. Horizontal scales below 1 km are poorly explored in the ocean, and simultaneous measurement of temperature and salinity in the mixed layer over this wide range of scales is, to our knowledge, unprecedented, although comparable measurements of temperature only have been made (*16*). We conducted a cruise from 23 January to 20 February 1997 in the subtropical gyre of the North Pacific along 140°W between 25°N and 35°N. We made observations with a SeaSoar (*17*) equipped with sensors to measure temperature, salinity, and pressure (*18*) in a series of tows. The SeaSoar was first towed in a sawtooth pattern between the pressure surfaces of 5 and 320 dbar. A complete cycle of the sawtooth was completed in 12 min or less, providing a

horizontal resolution better than 3 km at a tow speed of 4 m s^{-1}. The resulting high-resolution section of the upper ocean indicated a roughly 100-m-deep mixed layer overlying the thermocline (Fig. 1).

The second tow was made along the 50-dbar pressure surface, chosen to roughly bisect the mixed layer. Stable temperature and salinity measurements were possible at a frequency of 1 Hz, and thus the isobar tow allowed horizontal resolution down to 4 m. A newly designed control system enabled the SeaSoar to follow a constant pressure surface to a root-mean-square deviation of 0.3 dbar. The combination of fine horizontal resolution and accurate vertical control was essential to achieving the goal of this study. Additional

tows (not discussed further here) were made along the 200-dbar surface and the 24.8- and 25.5-kg m^{-3} isopycnals to investigate temperature-salinity variability on other surfaces in the upper ocean (*19*).

Data from the 50-dbar tow demonstrate that temperature and salinity in the mixed layer are strongly coherent over all length scales observed (Fig. 2). Temperature and salinity gradients coincide in such a way that density gradients are minimized—that is, fronts in the ocean tend to be warm and salty on one side and cold and fresh on the other. Remarkably, each temperature feature, no matter how small (the smallest scale visible in the bottom panel of Fig. 2 is on the order of 10 m), is mirrored in salinity. Compensa-
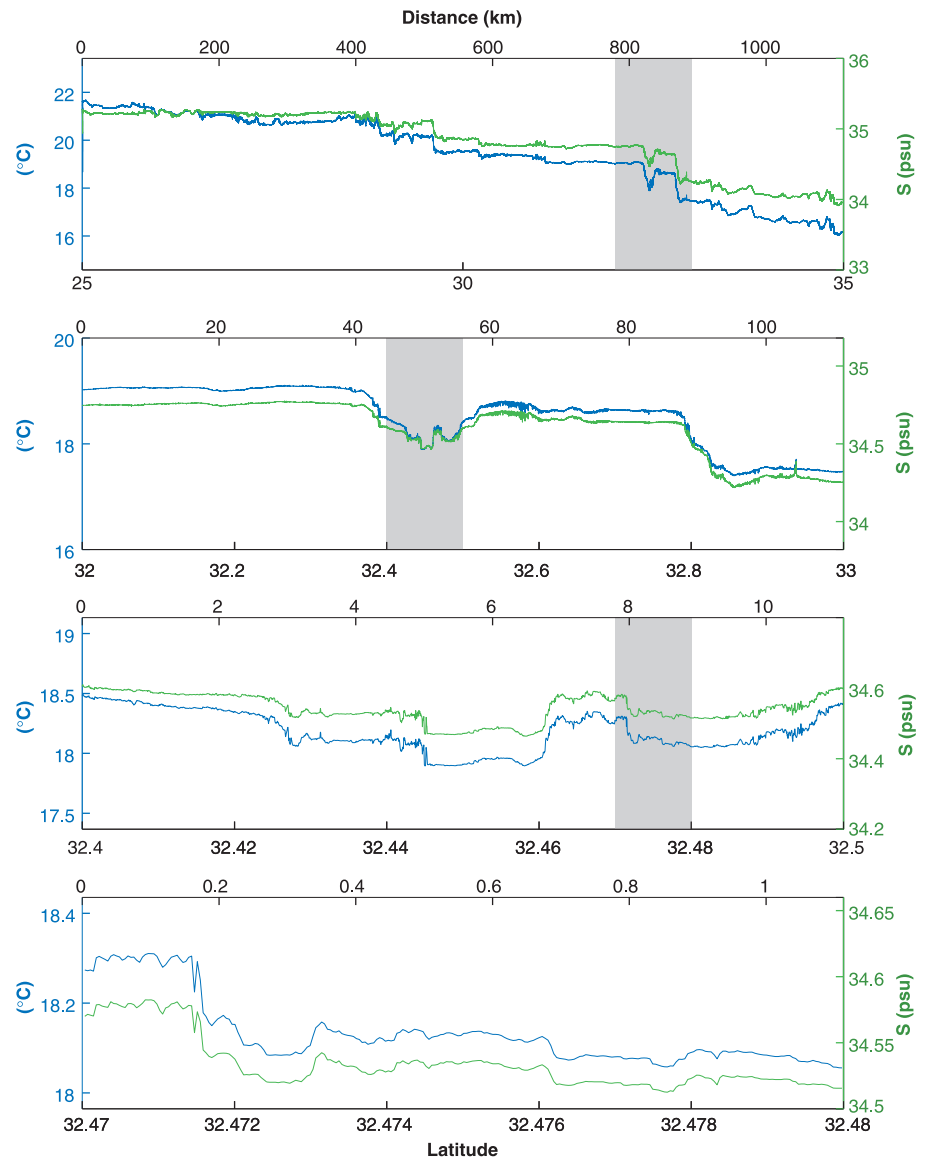
Fig. 2. Potential temperature θ and salinity *S* at 50 dbar. (**Top**) Potential temperature and salinity over the entire tow from 25°N to 35°N. Each succeeding panel is a magnification by a factor of 10 of the shaded region of the panel above. Note change in scale on the horizontal axis of each panel. Vertical axes are scaled by the thermal and haline expansion coefficients so that equal excursions of temperature and salinity imply identical effects on density. Temperature and salinity structure is compensated at all scales.

tion thus exists at all scales in these data, consistent with the Young model of density-driven shear dispersion. It is notable that strong density gradients are rarely observed even at the smallest scales. Apparently the process of slumping and mixing occurs so rapidly that we observe only the end result.

A suitable analysis technique for determining whether the compensation shown graphically in Fig. 2 is typical of all scales is the wavelet transform (20), which has the benefit of being both scale and location selective. The wavelet coefficients of temperature and salinity were calculated for wavelengths between 20 m and 10 km and are displayed as scatterplots (Fig. 3). A point in a scatterplot indicates the variability of temperature and salinity at a particular wavelength and location. The data have a slope close to 1 at all scales, indicating a tendency for compensation of temperature and salinity. Scatterplots such as these visually emphasize the outliers—that is, the largest fronts—whereas typical temperature and salinity gradients cluster near the origin. These plots thus show that the largest fronts at all scales have a density ratio near 1.

A consideration of two different measures of the density ratio helps to understand how R varies with scale and frontal strength. One measure of the density ratio for a given wavelength is the slope of the principal axis of the cloud of points in the scatterplot. The principal axis is found by minimizing a quadratic measure (the covariance between temperature and salinity) and is thus sensitive to the largest fronts. The slope of the principal axis for scales between 20 m and 10 km is a bit larger than unity at 1.1 to 1.4 (Fig. 4). A second measure of the typical density ratio is the median ratio of the wavelet coefficients of

temperature and salinity. The median is a robust estimator in the sense that it is less sensitive to outliers than is the principal axis. The median density ratio is less than the slope of the principal axis at all wavelengths (Fig. 4) because small gradients of temperature and salinity are less well correlated than are the largest gradients. Median R is near 1 at large scales and decreases abruptly at wavelengths shorter than 100 m. The decrease in median R occurs at scales shorter than the horizontal scale of the dominant turbulent eddies in the mixed layer (order 100 m). These turbulent eddies may be Langmuir cells (21, 22) driven by wind and surface waves, or connection cells driven by the surface buoyancy flux (23). Young's shear dispersion model is valid only at length scales larger than the turbulent eddy scale; at smaller scales the relationship between temperature and salinity should begin to break down.

Our results show that that the strongest temperature and salinity fronts tend to be compensated at all observed scales ranging from 20 m to 10 km. This result suggests that the mixed layer mixes horizontally in such a way that density gradients are dissipated while compensated temperature and salinity gradients persist. A horizontal diffusivity dependent on density gradient would produce this behavior, although we have not determined the specific functional dependence.

Our observations emphasize that, in the mixed layer, mixing activated by density gradients is more effective than mixing that homogenizes all tracers indiscriminately. This density gradient–driven mixing is symmetric with respect to temperature and salinity, and it is responsible for the tight correlation between fronts in the two trac-

ers. Most studies of the temperature-salinity relationship have focused on the asymmetry in the molecular diffusion of heat and salt (24). It has been argued that double diffusion is responsible for the vertical density ratio of 2 (where the spatial interval is vertical) observed in the ocean interior (25). However, double diffusion is unlikely to be important in the mixed layer where mechanical mixing is very strong. An open question is the role of double diffusion in modifying mixed-layer water as it is subducted into the thermocline.

A question that remains is whether our measurements in the North Pacific subtropical gyre are representative of other oceans. It is reasonable to assume that our observations on scales smaller than the Rossby radius of deformation (about 10 km) are universally valid. However, it is likely that the small density changes we observe on scales greater than 10 km are special to this region of the North Pacific. The observational fact remains that the large-scale density ratio is close to 2 (26). Iselin's observation that vertical profiles of temperature and salinity in the subtropical interior are coincident with meridional profiles in the winter mixed layer requires a large-scale density gradient. Our observations suggest a hypothesis that the temperature-salinity relationship of the winter mixed layer is staircase-like, with regions of $R = 1$ separated by confined regions of strong density gradients (27). The large-scale density ratio would thus be other than unity, but most thermohaline structure would be compensated. The question of what sustains the large-scale density ratio in the world's oceans remains open. External surface forcing is important, as the meridional gradient in surface heat flux dominates that in freshwater flux, and a large-scale R greater than 1 is

Fig. 3. Scatterplots of density variability due to temperature $\alpha\Delta\theta$ and salinity $\beta\Delta S$ at wavelengths of 10 km (**A**), 1 km (**B**), 100 m (**C**), and 20 m (**D**). Plotted are the wavelet coefficients of temperature and salinity each multiplied by the respective expansion coefficients. Dashed lines indicate a slope of 1. Scatterplots are close to a slope of 1, indicating a tendency for the density ratio to be 1 at these scales. Wavelet coefficients are calculated at 4-m increments and are serially correlated for the long wavelengths, as in (A) and (B), where the points are so closely spaced they appear to be lines.
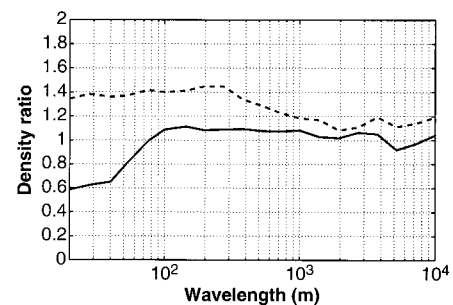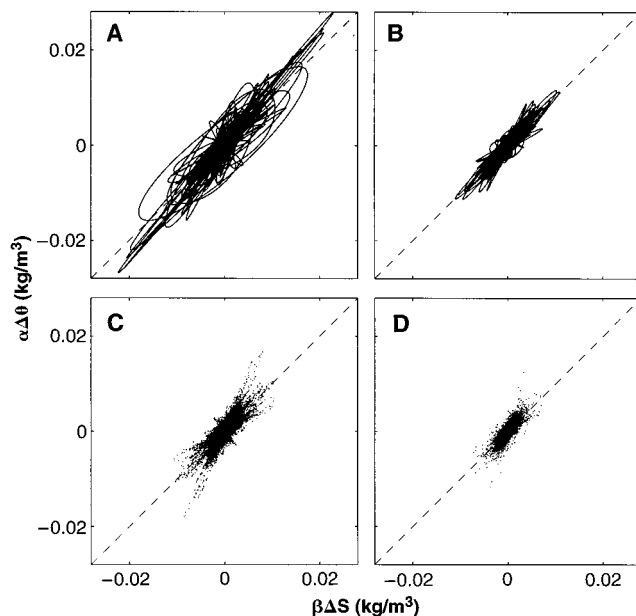
Fig. 4. Density ratio as a function of wavelength computed as a median (solid line) and as the slope of the principal axis (dashed line). Principal axis estimate of the density ratio, strongly influenced by the largest fronts, remains between 1.1 and 1.4. Median of the density ratio is near 1 at wavelengths down to 100 m. Below 100 m, the median decreases to 0.6 at the smallest resolved scales. Standard errors (calculated by a bootstrap technique) are ≤0.004 for the median and ≤0.01 for the slope of the principal axis.

expected (28). However, the ratio of heat to freshwater buoyancy fluxes is variable in large-scale maps (28) and in time series at a point (29), so internal ocean dynamics may be required to establish a uniform large-scale density ratio. Observational confirmation of our hypothesis of the existence of a staircase-like temperature-salinity relationship would require tows long enough to cross a number of strong density fronts and in different ocean basins.

References and Notes
1. C. O. D. Iselin, *Trans. Am. Geophys. Union* **20**, 414 (1939).
2. The mixed layer is a layer at the ocean's surface that is relatively vertically uniform in properties such as temperature and salinity. The turbulence that mixes this layer is a result of wind and surface cooling.
3. The thermocline is a region of relatively high stratification below the mixed layer.
4. H. Stommel, *Proc. Natl. Acad. Sci. U.S.A.* **76**, 3051 (1979).
5. J. R. Luyten, J. Pedlosky, H. Stommel, *J. Phys. Oceanogr.* **13**, 292 (1983).
6. M. C. Gregg, *J. Geophys. Res.* **94**, 9686 (1989).
7. J. R. Ledwell, A. J. Watson, C. S. Law, *Nature* **364**, 701 (1993).
8. G. I. Roden, *J. Phys. Oceanogr.* **5**, 557 (1975).
9. _____, *Ann. Geophys.* **2**, 399 (1984).
10. H. M. Stommel, *J. Phys. Oceanogr.* **23**, 142 (1993).
11. _____ and W. R. Young, *ibid.*, p. 151.
12. W. R. Young, *ibid.* **24**, 1812 (1994).
13. L. Chen and W. R. Young, *ibid.* **25**, 3064 (1995).
14. R. Ferrari and W. R. Young, *J. Mar. Res.* **55**, 1069 (1997).
15. The Earth's rotation should act to limit the slumping at horizontal scales larger than the Rossby radius of deformation (the scale above which the effects of rotation become important). Although slumping should occur at large scales, it need not proceed until isopycnals are horizontal.
16. R. M. Samelson and C. A. Paulson, *J. Geophys. Res.* **93**, 2237 (1988).
17. R. Pollard, *Nature* **323**, 433 (1986).
18. Sensors for measuring temperature and conductivity (which is used to calculate salinity) must be calibrated to account for differences in time constants of the sensors. We used the methods of Lueck and Picklo [R. G. Lueck and J. J. Picklo, *J. Atmos. Oceanic Technol.* **7**, 756 (1990)] and Rudnick and Luyten [D. L. Rudnick and J. R. Luyten, *J. Geophys. Res.* **101**, 923 (1996)].
19. Temperature-salinity variability below the mixed layer is caused by internal waves, stirring, and mixing. The isobar and isopycnal tows are intended to study these processes.
20. I. Daubechies, *Ten Lectures on Wavelets*, CBMS-NSF Regional Conference Series in Applied Mathematics (Society for Industrial and Applied Mathematics, Philadelphia, 1992); M. Farge, *Annu. Rev. Fluid Mech.* **24**, 395 (1992). The wavelet transform may be thought of as convolutions with a set of functions (wavelets) of changing frequency content. An important feature of a wavelet is that its quality factor Q, defined as the ratio of the wavelet's central wave number to its spread in wave number, is constant. Wavelets are derived by dilation of the so-called mother wavelet. Here we choose the Morlet wavelet (a plane wave modulated by a Gaussian envelope) with $Q = 2\sqrt{2}\pi$.
21. I. Langmuir, *Science* **87**, 119 (1938).
22. R. A. Weller *et al.*, *ibid.* **227**, 1552 (1985).
23. K. E. Brainerd and M. C. Gregg, *J. Geophys. Res.* **98**, 22645 (1993).
24. R. W. Schmitt, *Annu. Rev. Fluid Mech.* **26**, 255 (1994).
25. _____, *J. Phys. Oceanogr.* **11**, 1015 (1981).
26. L. G. Chen, *ibid.* **25**, 691 (1995). In winter between the 7° and 17°C isotherms, estimates of *R* are 1.9 averaged over the North Pacific and 1.4 at the longitude of our measurements (140°W).
27. Compensated temperature and salinity features are often found near strong density fronts [D. L. Rudnick and J. R. Luyten, *J. Geophys. Res.* **101**, 923 (1996)].
28. R. W. Schmitt, P. S. Bogden, C. E. Dorman, *J. Phys. Oceanogr.* **19**, 1208 (1989).
29. S. P. Anderson, R. A. Weller, R. B. Lukas, *J. Clim.* **9**, 3056 (1996).
30. We thank Lloyd Regier, Lyn Harris, and John Paoli for their efforts in support of the observational program. Thanks are due to Bill Young for inspiring discussions. We gratefully acknowledge the support of the National Science Foundation under grant OCE95-29752.

Transient Phase–Induced Nucleation

E. B. Sirota* and A. B. Herhold

A transient metastable rotator phase occurring on crystallization of hexadecane into its triclinic phase from the supercooled melt was directly observed with time-resolved synchrotron x-ray scattering. In this system, the limit of supercooling (the crystallization temperature) is determined by the thermodynamic stability of the transient phase with respect to the liquid. The crystallization kinetics of the homologous series of n-alkanes was measured and explained in terms of a crossover from stability to "long-lived" metastability to transient metastability. This crossover allowed further confirmation of the nature of the transient phase.

Materials often crystallize into metastable forms when cooling from the melt. Once formed, a metastable phase may remain stable indefinitely even for very large undercoolings. However, nucleation could occur to create a transient phase that converts to the stable form during some stage of growth. In such a case, there may be no temperature at which the metastable phase will remain indefinitely. Transient phases are intrinsically difficult to observe and their study has been limited (1–3). Such transient states are not only intermediate forms on the path to the final state (4) but they can be key to understanding the crystallization behavior. In particular, the nucleation temperature of the transient state can determine the observed crystallization or precipitation temperature of the stable phase, that is, the limit of supercooling. In addition, the properties of the metastable phase can determine the growth morphology of the crystal; for example, enhanced chain mobility in the metastable hexagonal phase (which is stable at high pressure) may cause lamellar thickening in polyethylene (3).

The n-alkanes (C_nH_{2n+2}, abbreviated C_n) are not only interesting in their own right because of their varied behavior but are the principal component of petroleum waxes and the building block of many derivative molecules whose properties are strongly influenced by their alkyl component (5, 6). The n-alkanes exhibit an even-odd effect in their melting points and crystal structures (5, 7, 8), but the

kinetics and observed hysterisis have remained unexplained. Here we show that the stability of the transient phase can be optimized for an appropriate choice of alkane chain length. We provide an example of transient phase–induced nucleation and explain the kinetic behavior of n-alkane crystallization in terms of a crossover from "long-lived" to transient metastability.

In general, alkanes exhibit rotator phases below the melting temperature (6, 9, 10). For *n*-even alkanes, in the equilibrium phase diagram the rotator (R) phases are replaced at lower *n* by a triclinic (T) nonrotator crystal phase. Bulk melts of the *n*-odd alkanes ($15 \leq n \leq 29$) exhibit a liquid-rotator (L→R) transition with negligible supercooling (7, 8, 10). The lack of supercooling in the melts has been suggested (8, 11) to be related to the presence of a surface monolayer R phase that occurs in equilibrium at the liquid-vapor interface a few Celsius degrees above the crystallization temperature (12), and this surface R phase would serve as an ideal nucleation site for the bulk R phase (13). The equilibrium melting points exhibit a significant even-odd effect that can be associated with whether melting occurs from the T crystal (*n*-even) or from the R phase (*n*-odd) (7, 8). However, the even-odd effect disappears when observed freezing temperatures are considered (Fig. 1) because the *n*-even alkanes with high melting points supercool, whereas the *n*-odd alkanes, which crystallize into the R phase, do not. Is it a coincidence that the amount of supercooling for *n*-even alkanes is equal and opposite to the even-odd difference in the melting temperatures? It had been hypothesized that it is not (8). We now demonstrate this correspondence experimentally and show that short *n*-even alkanes crystallize through a transient R phase.

Exxon Research and Engineering Company, Corporate Research Science Laboratory, Route 22 East, Annandale, NJ 08801, USA.

*To whom correspondence should be addressed. E-mail: ebsirot@erenj.com